Turkish Journal of Science & Technology
18(1), 131-138, 2023

Research Paper
https://doi.org/10.55525/tjst.1209085

Variation of Electrical Resistivity During Magnetic Field-Induced Martensitic Transformation in Vanadium added NiMnSnB alloys

Gökhan KIRAT[1*],
[1] Scientific and Technological Research Center, Inönü University, Malatya, Türkiye
[*1] gokhan.kirat@inonu.edu.tr

(Geliş/Received: 23/11/2022; Kabul/Accepted: 10/02/2023)

Abstract: In this study, the structural and electrical properties of $Ni_{49-x}V_xMn_{37}Sn_{12}B_2$ (x = 0, 1, 2, and 3) ferromagnetic shape memory alloys were investigated. According to XRD analyzes at room temperature, the x=0 sample was in the martensite phase, the x=1 and 2 samples were in the mixture phase, and the x=3 sample was in the austenite phase. The resistivity analyses depend on temperature showed that all samples exhibited martensitic transformation and the phase transformation temperature decreased with V doping. Magnetoresistance (MR) values were calculated using ρ-T curves performed under 0 T and 1 T magnetic fields. The observed negative MR is consistent with Kataoka's s-d model. A_s-A_f interval was determined and M-H measurements were made at constant temperatures determined in this interval. The results were attributed to the magnetic field-induced phase transformation (MFIPT). In order to examine the effects of MFIPT on the electrical resistivity, the resistivity depend on magnetic field was measured using the same thermal process. The overlapping of the curves in the high magnetic field revealed that the resistivity decreased due to the MFIPT as well as the MR.

Key words: Magnetoresistivity, martensitic transformation, magnetic field induced structural transformation.

Vanadyum Eklenmiş NiMnSnB Alaşımlarında Manyetik Alan Kaynaklı Martensitik Dönüşüm Sırasında Elektrik Direncinin Değişimi

Öz: Bu çalışmada $Ni_{49-x}V_xMn_{37}Sn_{12}B_2$ (x = 0, 1, 2, and 3) ferromanyetik şekil hatırlamalalı alaşımların yapısal ve elektriksel özellikleri incelenmiştir. Oda sıcaklığındaki XRD analizine göre x=0 numunesi martensit fazında, x=1 ve 2 numunesi karışım fazında ve x=3 numunesi östenit fazındadır. Sıcaklığa bağlı özdirenç analizleri bütün numunelerin martensitik dönüşüm sergilediğini ve faz dönüşüm sıcaklığının V katkılamasıyla azaldığını göstermiştir. 0 T ve 1 T manyetik alan altında gerçekleştirilen ρ-T eğrileri kullanılarak manyetodirenç (MR) değerleri hesaplanmıştır. Gözlemlenen negatif MR, Kataoka nın s-d modeli ile uyumludur. A_s-A_f aralığı belirlenmiştir ve bu aralıkta belirlenen sabit sıcaklıklarda M-H ölçümleri yapılmıştır. Sonuçlar manyetik alan kaynaklı faz dönüşümüne atfedilmiştir (MFIPT). MFIPT 'in elektrik özdirenci üzerindeki etkilerini incelemek için, aynı termal süreç kullanılarak manyetik alana bağlı özdirenç ölçülmüştür.Yüksek manyetik alanda eğrilerin üst üste binmesi, MR'ın yanı sıra MFIPT 'e bağlı olarak direncin azaldığını ortaya koymuştur.

Anahtar kelimeler: Manyetodirenç, martensitik dönüşüm, manyetik alan kaynaklı yapısal dönüşüm.

1. Introduction

The martensitic transformation (MT) is a first-order structural phase transition in the solid state without any diffusion. During the MT, the high temperature phase, which is called austenite, transforms into the low temperature phase, which is called martensite [1]. Shape memory effect (SME) is an important property of some alloy groups that exhibit martensitic transformation. The most important characteristic feature of shape memory alloys (SMA) is that they regain their original shape when they transform to the austenite phase after being deformed by stress in the martensite phase [2]**.** In addition, SMA have useful mechanical properties such as excellent corrosion resistance and superelasticity [3]. Therefore, in recent years, SMA have been the subject of many scientific studies and also they have been using extensively in the a lot of industrial applications. Some instances of these applications are stents, eyeglass frames, sensitive thermal sensors, microactuators, electronic devices, magnetic field sensors, valves and medical devices [4].

In the conventional SMA, shape recovery is usually triggered by heat, whereas in ferromagnetic shape memory alloys (FSMA) it can be controlled by magnetic field as well as heat [4]. The obtained higher strain depends on the applied magnetic field compared to traditional actuator materials like piezoelectric and magnetostrictive materials increases the interest in FSMA. For example, while a strain of <0.2% can be obtained under approximately 60 MPa stress and 0.3 T magnetic field in

[*] Corresponding author: gokhan.kirat@inonu.edu.tr ORCID Number of author: [1] 0000-0001-7357-2921

magnetostrictive Terphenol-D material, up to 10% magnetic field-induced strain can be obtained in FSMA [5]. Two different mangetic field induced strain (MFIS) mechanisms can occur in the FSMA as a result of applying an external magnetic field. The first is the magnetic field-induced martensitic twin variant reorientation (MIR), and the second is the magnetic field-induced structural phase transformation. The former mechanism, MIR is the rearrangement of the microstructure without a change in the crystalline structure as a result of twin boundary motion triggered by the external magnetic field (Fig 1.a.). If the magnetocrystalline anisotropy energy (MAE) of a martensite variant is larger than the energy required for twin boundary motion, MAE acts as a driving force for MIR. The MAE is determined from the difference between the magnetizations along the easy and hard axes of the ferromagnetic single martensite variant (Fig 1.b.). Another possible mechanism for inducing MFIS is magnetic field-induced structural phase transformation (MFIPT). In this mechanism, the crystal structure transforms from martensite to austenite by increasing the external magnetic field at a certain temperature where both phases (austenite and martensite) should be coexist (Fig 1.c.) [6]. The difference in Zeeman energies of the present phases is the driving force for MFIPT and the difference must be higher than the energy required to move the phase boundaries (Fig 1.d.). If the external magnetic field is shown by $\mu_0 H$ and the magnetization difference between the transformation phases is given by ΔM, Zeeman energy can expressed as $E_{\text{zeeman}} = \mu_0 H \Delta M$ [7].

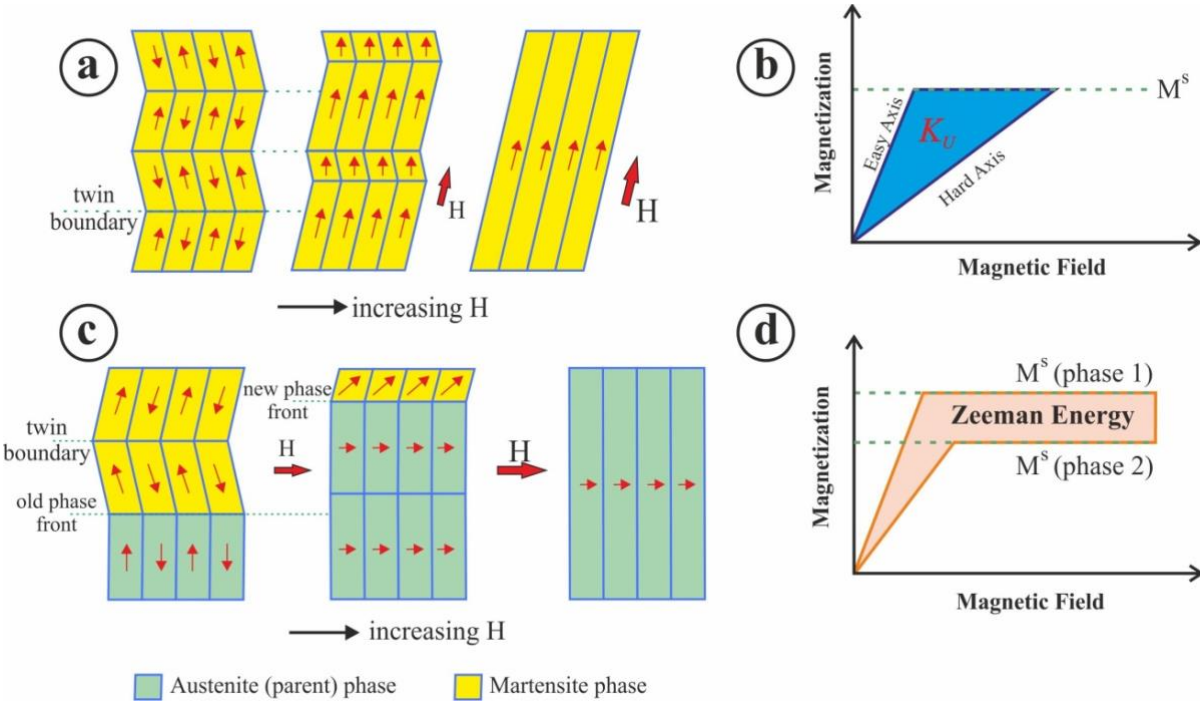

Figure 1. (a) Effect of increasing external magnetic field on MIR (b) MAE(K_u) responsible for MIR (c) Effect of increasing external magnetic field on MFIPT (d) Zeeman energy difference between austenite and martensite phases responsible for MFIPT [5, 6]

In recent years, researchers have carried out a lot of notable research about MFIPT. In most of these studies, they have aimed to explain the MFIPT mechanism by determining the magnetic moment of the material during the field-induced structural phase transformation. In addition, various transition metal doping are made to improve the magnetic properties of Ni-Mn based alloys. In this study, it is desired to reach high magnetic moment value by adding Vanadium to the NiMnSn alloy system. The goals of the current study are (i) to investigate the magnetoresistance properties of vanadium (V) doped NiMnSnB alloys and (ii) to determine the resistance variation due to the magnetic field change during MFIPT.

2. Experimental

$Ni_{49-x}V_xMn_{37}Sn_{12}B_2$ (x = 0, 1, 2, and 3) (at. %) ferromagnetic shape memory Heusler alloys were produced as ingots form by arc-melting furnace using pure Ni, V, Mn, Sn and B (purities higher than 99.99%) powders. The melting process was carried out by creating plasma in an argon atmosphere and flowing a current of ~150 A throughout the samples. In order to obtain homogeneous samples, the melting process was repeated several times by turning the samples. The fabricated samples were heat treated at 900 °C for 48 h to ensure homogenization, and then quenched in ice-water. To prevent the oxidation during heat treatment, the samples were placed in the vacuumed quartz tube. The samples were marked as V0 (x=0), V1 (x=1), V2 (x=2) and V3 (x=3), respectively. The crystal structures at room temperature (RT) were determined with the “Rigaku Miniflex

600" computer-controlled X-ray diffractometer using CuKα (λ=1.5405 Å) radiation. The electrical resistivity measurements were performed with the AC Transport attachment of the Quantum Design PPMS device. Martensitic transformation temperatures were determined by means of temperature-dependent resistivity measurements. Then, magnetoresistivity measurements were carried out at different temperatures determined between the austenite start (A_S) and austenite finish (A_f) temperatures of each sample. It should be noted that the temperature was kept constant during these measurements and the samples were cooled until they completely transform to the martensite phase before each measurement. Magnetic field-dependent magnetization (M-H) curves were determined by the vibrating sample magnetometer (VSM) with using the same thermal process.

3. Results and Discussions

As discussed above, a first-order structural phase transition occurs between the austenite and martensite phases during MT. While the austenite phase usually has a cubic $L2_1$ crystal structure, the martensite phase may have monoclinic 10*M* and 14*M*, orthorhombic 4*O* or unmodulated double tetragonal $L1_0$ crystal structures depending on the composition and temperature [8–11]. XRD patterns of the V0, V1, V2 and V3 samples at RT are shown in Fig. 1. Peaks of monoclinic 10*M* and orthorhombic 4*O* crystal structures were obtained in the V0 sample, whereas no peaks from the cubic structure were detected. Based on this result, it can be expected that the sample in the martensite phase at RT. In addition to the peaks of 10*M* and 4*O*, the V1 sample has cubic (220) peaks due to the presence of the austenite phase. Except for the cubic (220), (222), (400) and (422) peaks, only the (221) peak of the 4*O* phase was observed in the V2 sample. Therefore, it can be expected that the ratio of the austenite phase in the V2 sample at room temperature is higher than in the V1 sample. The detection of only the peaks of the cubic structure in the V3 sample shows that the sample is completely in the austenite phase at RT. The lattice parameters of all samples refined by the least-squares method and the final compositions of the samples analyzed by the Energy Dispersive X-Ray Analysis(EDX) method were listed in Table 1.

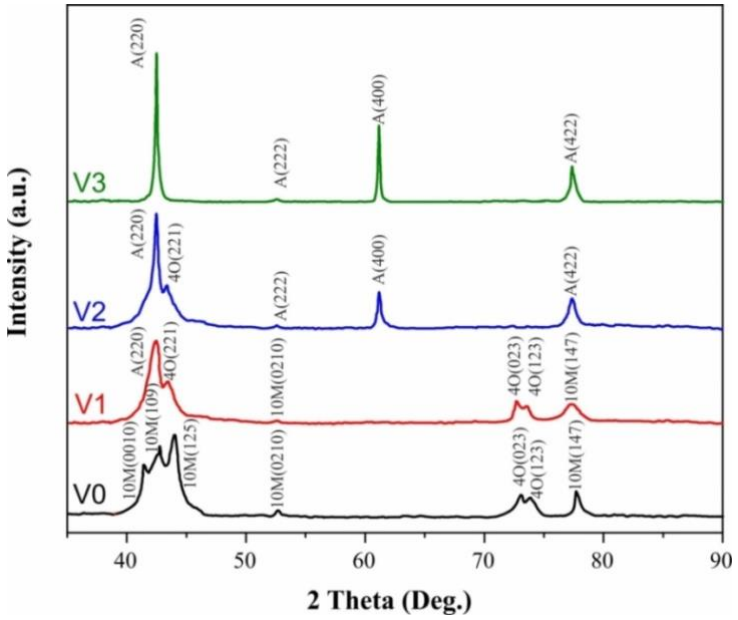

Figure 2. XRD patterns of V0, V1, V2 and V3 samples at room temperature

Table 1. Crystal structures, lattice parameters and final composition (determined by EDX) at RT of the V0, V1, V2 and V3 samples.

Sample	Nominal composition (at. %)	Final composition (at. %)	Crystal structure	Lattice parameters		
				a(nm)	b(nm)	c(nm)
V0	$Ni_{49}Mn_{37}Sn_{12}B_2$	$Ni_{49.2}Mn_{36.1}Sn_{14.7}+B_y$	10*M*	0.4337	0.5660	2.1968
			4*O*	0.4431	0.5702	0.8795
V1	$Ni_{48}V_1Mn_{37}Sn_{12}B_2$	$Ni_{48.1}V_{1.2}Mn_{36.3}Sn_{14.4}+B_y$	4*O*	0.4424	0.5693	0.8786
			$L2_1$	0.6014	0.6014	0.6014
V2	$Ni_{47}V_2Mn_{37}Sn_{12}B_2$	$Ni_{47.1}V_{2.1}Mn_{36.2}Sn_{14.6}+B_y$	$L2_1$	0.6011	0.6011	0.6011
V3	$Ni_{46}V_3Mn_{37}Sn_{12}B_2$	$Ni_{46.0}V_{3.6}Mn_{36.4}Sn_{14.0}+B_y$	$L2_1$	0.6010	0.6010	0.6010

Since Heusler alloys are one of the rare examples of ferromagnetic alloys whose resistance exceeds the critical Mooij value, investigation of their magneto-transport properties provides interesting results [12]. According to Mooij's rule, the resistivity should decrease with increasing temperature when the resistivity of the alloy exceeds 150μΩcm, regardless of the scattering mechanism of the charge carriers. The resistivity of Heusler alloys is can suitable to this rule, while it can be similar to metallic behavior, depending on the composition of the alloy [13–16].

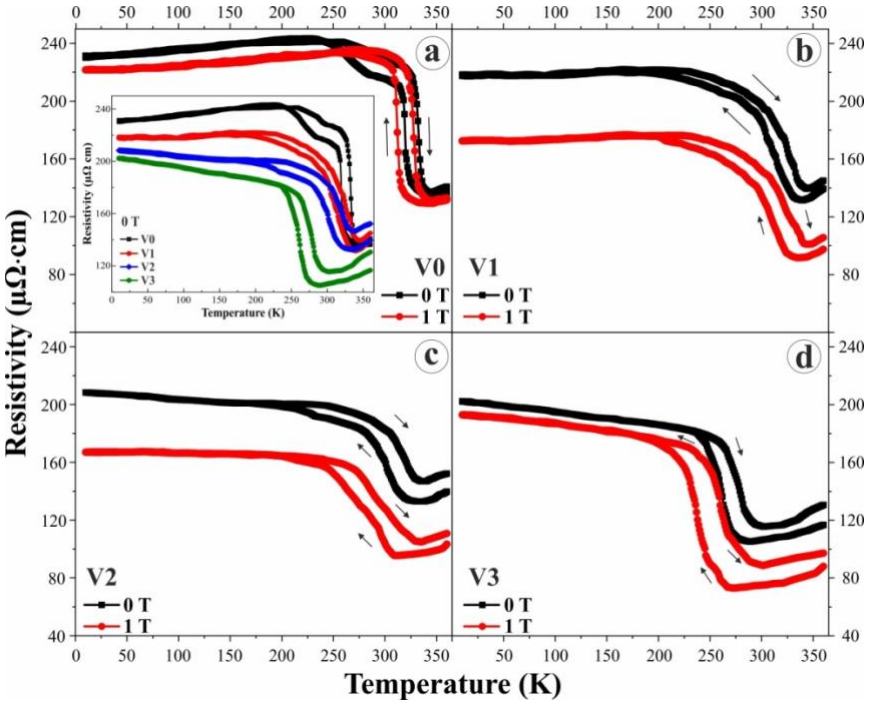

Figure 3. ρ-T curves of (a)V0, (b)V1, (c)V2 and (d)V2 at 0T and 1T

The resistivity vs temperature curves of $Ni_{49-x}V_xMn_{37}Sn_{12}B_2$ (x = 0, 1, 2, and 3) alloys are given in Figure 3. Resistivity measurements were performed both without a magnetic field and under 1 T external magnetic field. One of the ways to the characterization of martensitic transformation is the sudden resistance changes obtained in the temperature-dependent resistance curve. The abrupt changes due to MT have been clearly detected in the resistivity curves of all samples. This jumplike difference between the resistances of martensite and austenite phases can originate owing to two reasons. (i) A sudden change in the density of states at the fermi energy level (ii) a change in the order parameter of the crystal structure. In the studies carried out to calculate the normal hall effect coefficient, no jump in the state density of the fermi energy level was observed around the martensitic transformation temperature. Therefore, it can be expect that the dominant mechanism in the resistance change during MT is the variation in the structural order parameter [17]. Evidently, both the phase transition temperatures (table 2) and the resistivity values (inset of Fig.3.a) decreased by increasing the amount of V. In addition, a more gradual phase transition was observed with increasing doping amount. It is clearly seen that especially in V0 and V1 samples, the temperature dependence of the martensite phase is relatively weak which is typical behavior of high resistivity metals. This is because scattering by phonons and magnetic heterogeneities is negligible and scattering originating from increasing disorder is more dominant in the scattering mechanism [17]. The resistivity of martensite phase of V0 and V1samples, during cooling, firstly increased slightly and then started to decrease around 225 K and 175 K, respectively. The increase in resistivity in this temperature range (T<225K for V0, T<175K for V1) has been attributed to scattering by magnetic inhomogeneities [18]. The resistivity value in the martensite phase of V2 and V3 samples increased continuously with decreasing temperature in accordance with Mooij's rule. ρ-T measurements performed under an external magnetic field of 1 T revealed that both the phase transition temperature and the resistivity value decreased. The shift in phase transformation temperatures with application of a magnetic field is described by the Clausius-Clapeyron equation[19];

$$\frac{\Delta H}{\Delta T} = -\frac{Q}{T_M \Delta M}, \ \Delta S = -\frac{Q}{T_M} \tag{1}$$

where Q indicates the evolved heat of transformation, TM represents MT temperatures and ΔM shows the magnetization difference between austenite and martensite phases.

Table 2: Martensite start (M_s), martensite finish (M_f), austenite start (A_s) and austenite finish (A_f), of the V0, V1, V2 and V3 samples.

Sample	Mag. Field	M_s (K)	M_f (K)	A_s (K)	A_f (K)
V0	0 T	325.5	307.6	325.0	342.1
	1 T	315.8	304.3	320.1	333.0
V1	0 T	324.5	276.8	295.0	340.5
	1 T	316.9	271.9	291.2	332.4
V2	0 T	319.6	274.1	292.9	331.4
	1 T	307.8	236.6	262.8	324.5
V3	0 T	276.8	249.5	262.9	291.8
	1 T	250.5	225.3	245.7	274.1

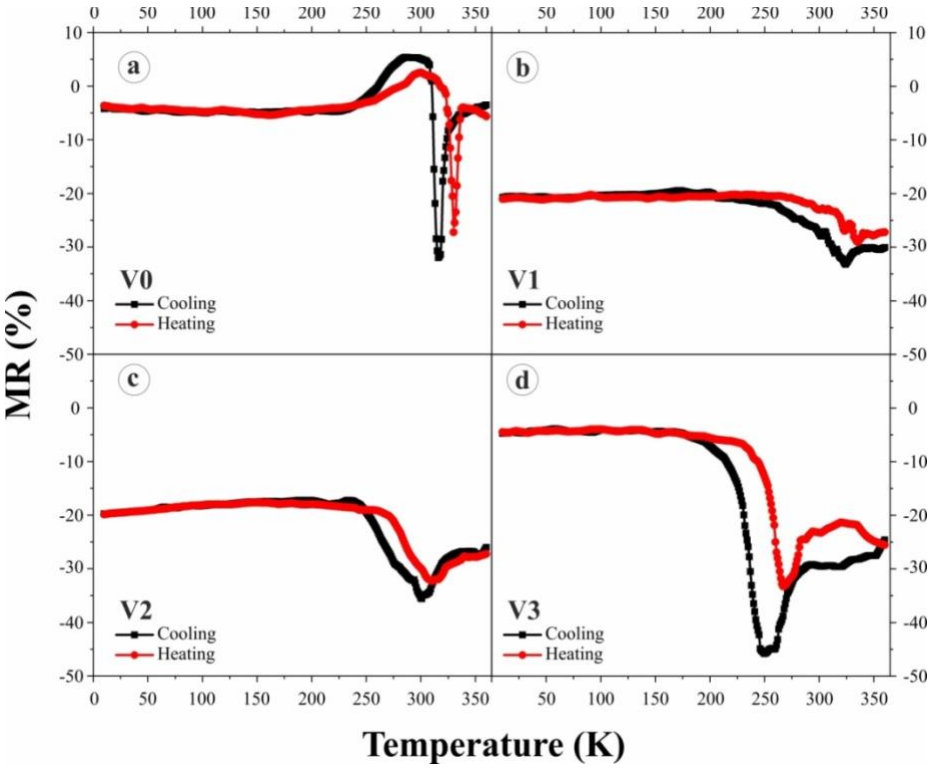

Figure 4. Magnetoresistivity curves of (a)V0, (b)V1, (c)V2 and (d)V2 during cooling and heating

Figure 4 shows temperature dependence magnetoresistivity (MR) in the magnetic field of 1 T which is calculated from;

$$MR(\%) = \frac{[\rho(H) - \rho(0)]}{\rho(H)} 100(\%) \quad (2)$$

equation. MR has a negative value for all alloys. The negative MR generated by the application of the magnetic field in ferromagnetic materials was explained by Kataoka using the s-d model. This model is based on the principle that s-conduction electrons are scattered by localized d spins. In addition, the MR increased with increasing V doping and the highest MR values in the magnetic field of 1 T are -31.7%, -33.2%, -35.2% and -45.6%, respectively. The resistivity of the martensite phase increases because of scattering from various orientations of the twin boundaries and residual resistivity. With the application of the magnetic field, the MT temperature shifts to a lower temperature. Also, the structural transition to the martensite phase, which has the lower symmetry, is accompanied by modulation, which increases the scattering of conduction electrons. Coexistence of all these effects leads to higher negative MR [20, 21]. Moreover, MR values obtained in the cooling process

are higher than in the heating process. The obtained MR values in the current study exhibit very successful results when compared with the literature [2, 22, 23].

Figure 5 shows the thermomagnetization curves at 5 different temperatures in the A_s-A_f range determined from Table 2 for each sample. Before each measurement, the samples were cooled until they were completely transformed into the martensite phase. Metamagnetic behavior attributed to magnetic field-induced structural transformation was detected in all samples. Martensite and austenite phases coexist in the A_s-A_f range and with increasing temperature, the martensite ratio decreases while the austenite ratio increases. With the application of a magnetic field to the sample in this temperature region, the magnetization of the austenite phase, which has stronger ferromagnetic interactions, increases suddenly, whereas the magnetization of the weak magnetic martensite phase increases more slowly. Simultaneously, structural transformation occurs from martensite to the austenite phase with the rising magnetic field. When a critical magnetic field level is reached, the sample completely transforms into the austenite phase and after that, the sample remains in the austenite phase even if the magnetic field is reduced. Consequently, a hysteresis occurs between the curves obtained by increasing and decreasing the magnetic field. The hysteresis as a result of metamagnetic behavior have been provide clear evidence for MFIPT [23–29].

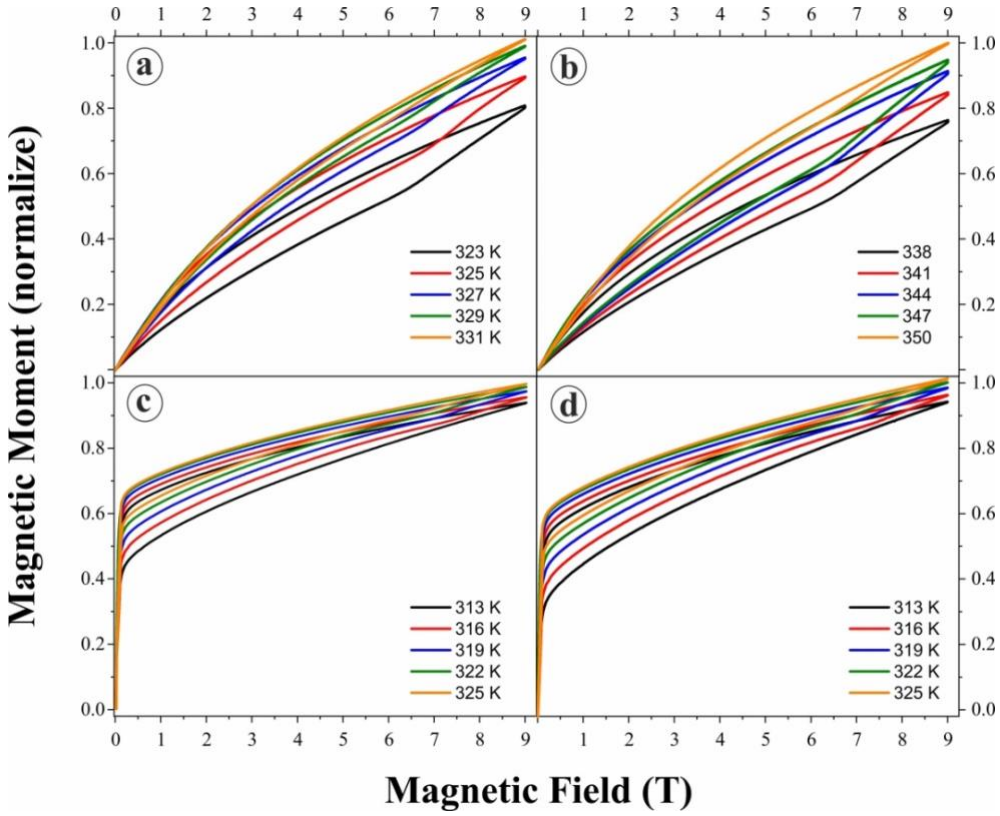

Figure 5. (color online) M-H curves of (a)V0, (b)V1, (c)V2 and (d)V2 at different temperatures determined in the range of A_s and A_f

In order to determine the change in electrical resistance during MFIPT, the same thermal process as the thermomagnetization analyzes was applied, and resistance measurements depending on the magnetic field were carried out. The results are given in figure 6. It should be noted that each measurement was carried out at a constant temperature and beforehand the samples were cooled until they transform into the martensite phase. In these measurements carried out at a constant temperature, it is clearly seen that the resistivity decreases as the temperature increases when focusing on the resistivity values at 0 T magnetic field. This is the opposite of what is expected from the metallic behavior and it is owing to the higher proportion of the martensite phase, which has higher resistivity, at low temperatures. The resistivity decreased with increasing magnetic field and the curves overlapped at approximately 8-9 T magnetic field. The negative magnetoresistance behavior of ferromagnetic Heusler alloys was discussed above. Although the decrease in resistivity with an increasing magnetic field can be partially explained by the MR effect, MR is insufficient to explaining the difference between the resistance values at 0 T and the overlapping of the curves at the high magnetic field. The transition from the higher resistive martensite phase to the lower resistive austenite phase can explain the reduction in resistivity with an increasing magnetic field. Moreover, the structural transformation can account for the overlapping of the curves in a high magnetic field. Therefore, it can be anticipated that the resistivity behavior depending on the magnetic field from Figure 6 is a result of the structural phase transformation as well as the MR. Additionally, these results are in accordance with the M-H curves shown in Fig. 5.

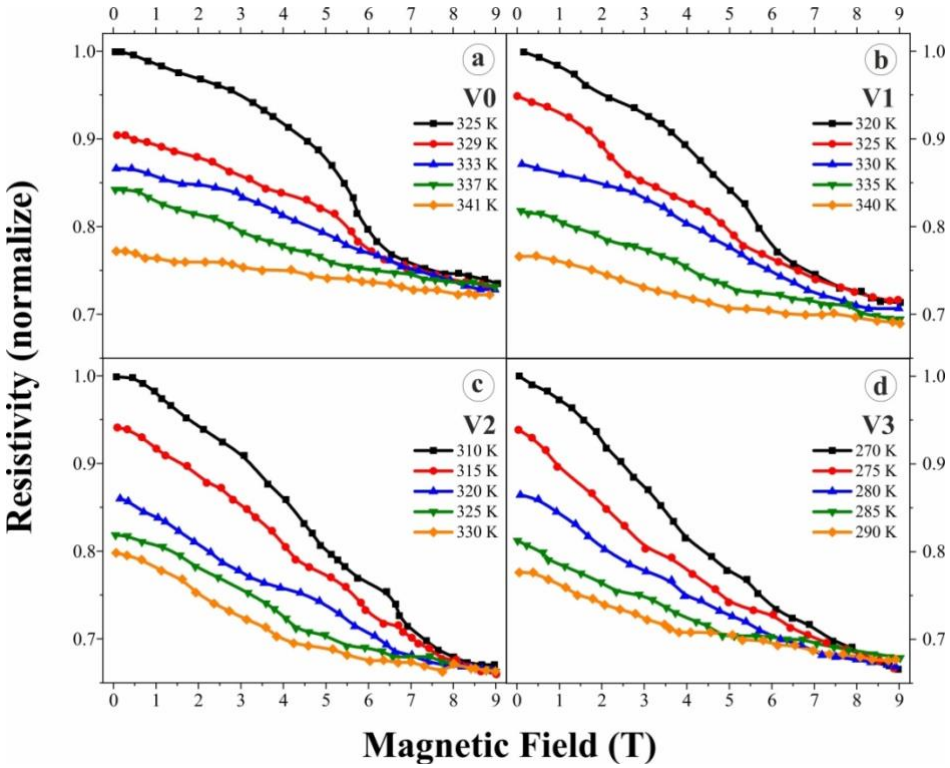

Figure 6. ρ-H curves of (a)V0, (b)V1, (c)V2 and (d)V2 at different temperatures determined in the range of A_s and A_f

4. Conclusion

In the present study, the structural and electrical properties of $Ni_{49-x}V_xMn_{37}Sn_{12}B_2$ (x = 0, 1, 2, and 3) alloys produced by the arc melting were investigated in detail. XRD patterns showed that the V0 sample has the 4*O* and 10M structures coexist at RT. V1 has $L2_1$ cubic structure in addition to 4*O* and 10M. The martensite content decreased in the V2 sample and only cubic $L2_1$ structure was detected in the V3. The all samples exhibited martensitic transformation around RT. The phase transition temperature and electrical resistivity value decreased with doping. MT temperatures shifted to lower temperatures by applying an external magnetic field, which the Clausius-Clapeyron equation explains. The magnetoresistivity was calculated using equation 2 and it was determined that increasing the magnetic field decreases the resistivity. It was confirmed that the samples exhibited MFIPT by M-H measurements performed at the determined constant temperatures in the A_s-A_f interval. Electrical resistivity analyzes were carried out during MFIPT using the same thermal process as the M-H measurements. In the measurements made at different temperatures, the resistivity decreased with increasing magnetic field and the curves overlapped in the high field. These obtained curves reveal the variation characteristic of electrical resistance during MFIPT.

References

[1] Pérez-Landazábal JI, Recarte V, Sánchez-Alarcos V, Gómez-Polo, C, Kustov S, Cesari E. Magnetic field induced martensitic transformation linked to the arrested austenite in a Ni-Mn-In-Co shape memory alloy. J Appl Phys 2011; 109(9), 093515-093521.

[2] Han ZD, Wang DH, Zhang CL, Xuan HC, Zhang JR, Gu BX, Du YW. The phase transitions, magnetocaloric effect, and magnetoresistance in Co doped Ni-Mn-Sb ferromagnetic shape memory alloys. J Appl Phy 2008; 104(5), 053906-0539012.

[3] Desroches R, Smith B. Shape memory alloys in seismic resistant design and retrofit: A critical review of their potential and limitations. J Earthq Eng 2004;. 8, 415–429.

[4] Kirat G. Exchange Bias Effect in NiMnSbB Ferromagnetic Shape Memory Alloys Depending on Mn Content. Adyu J Scı 2021; 11, 444–455.

[5] Karaca HE, Karaman I, Basaran B, Lagoudas DC, Chumlyakov YI, Maier HJ. On the stress-assisted magnetic-field-induced phase transformation in Ni_2MnGa ferromagnetic shape memory alloys. Acta Mater 2007; 55, 4253–4269.

[6] Karaca HE, Karaman I, Basaran B, Ren Y, Chumlyakov I, Maier HJ. Magnetic Field-Induced Phase Transformation in NiMnCoIn Magnetic Shape-Memory Alloys — A New Actuation Mechanism with Large Work Output. Adv Funct Mater 2009; 19, 983–998.
[7] Zhang H, Zhang X, Qian M, Yao Z, Wei L, Geng L. Increasing working temperature span in Ni-Mn-Sn-Co alloys via introducing pores. J Magn Magn Mater 2000; 500, 166359-166362.
[8] Zheng H, Wang W, Xue S, Zhai Q, Frenzel J, Luo Z. Composition-dependent crystal structure and martensitic transformation in Heusler Ni-Mn-Sn alloys, Acta Mater 2013; 61, 4648–4656.
[9] Kirat G, Aksan MA. Influence of the Cu substitution on magnetic properties of Ni–Mn–Sn–B shape memory ribbons. Appl Phys A-Mater 2021; 127, 1–9.
[10] Pons J, Chernenko VA. Santamarta R, Cesari E. Crystal structure of martensitic phases in Ni-Mn-Ga shape memory alloys, Acta Mater 2000; 48, 3027–3038.
[11] Deltell A, Escoda L, Saurina J, Suñol J. Martensitic Transformation in Ni-Mn-Sn-Co Heusler Alloys. Metals 2015; 5, 695–705.
[12] Titov IS, Zhukov AP, Gonzalez J, Kazakov AP, Dubenko IS, Granovskii AB, Pathak AK, Perov NS, Prudnikov VN, Ali N. Hall effect in a martensitic transformation in Ni-Co-Mn-In Heusler alloys. JETP Lett 2011, 92, 666–670.
[13] Guha S, Datta S, Panda SK, Kar M. Critical Behavior and Magnetocaloric Effect in Co_2CrAl Heusler Alloy. Physica Status Solidi (B): Basic Res 2022; 259, 2100533-2100541.
[14] Blinov M, Aryal A, Pandey S, Dubenko I, Talapatra S, Prudnikov V, Lähderanta E, Stadler S, Buchelnikov V, Sokolovskiy V, Zagrebin M, Granovsky A, Ali N. Effects of magnetic and structural phase transitions on the normal and anomalous Hall effects in Ni-Mn-In-B Heusler alloys. Phys Rev B 2020; 101, 94423-94429.
[15] Pandey S, Blinov M, Aryal A, Dubenko I, Prudnikov V, Lähderanta E, Granovsky A, Kazachkova N, Stadler S, Ali N. Drastic violation of the basic correlation between the Hall effect and resistivity in the Heusler alloy $Ni_{45}Cr_5Mn_{37}In_{13}$, . J Magn Magn Mater 2019; 481, 25–28.
[16] Sivaprakash P, Arumugam S, Esakki Muthu S, Raj Kumar DM, Saravanan C, Rama Rao NV, Uwatoko Y, Thiyagarajan R. Correlation of magnetocaloric effect through magnetic and electrical resistivity on Si doped Ni–Mn–In Heusler melt spun ribbon. Intermetal 2021; 137, 107285-107293.
[17] Zhukov AP, Prudnikov VN, Dubenko IS, Granovskii AB, Kazakov AP. Determination of the normal and anomalous hall effect coefficients in ferromagnetic $Ni_{50}Mn_{35}In_{15-x}Si_x$ Heusler alloys at the martensitic transformation. J Exp Theor Phys+ 2012; 115, 805–814.
[18] Prudnikov VN, Kazakov AP, Titov IS, Perov NS, Granovskii AB, Dubenko IS, Pathak AK, Ali N, Zhukov AP, Gonzalez J. Hall effect in a martensitic transformation in Ni-Co-Mn-In Heusler alloys. JETP Lett 2010; 92, 666–670.
[19] Pasquale M, Sasso CP, Lewis LH, Giudici L, Lograsso T, Schlagel D, Magnetostructural transition and magnetocaloric effect in $Ni_{55}Mn_{20}Ga_{25}$ single crystals. Phys Rev B 2005; 72, 1–5.
[20] Singh S, Biswas C. Magnetoresistance origin in martensitic and austenitic phases of $Ni_2Mn_{1+x}Sn_{1-x}$, Appl Phys Lett 2021; 98, 212101-212104.
[21] Biswas C, Rawat R, Barman SR. Large negative magnetoresistance in a ferromagnetic shape memory alloy: $Ni_{2+x}Mn_{1-x}Ga$. Appl Phys Lett 2005; 86, 1–3.
[22] Xuan HC, Zheng YX, Ma SC, Cao QQ, Wang DH, Du YW. The martensitic transformation, magnetocaloric effect, and magnetoresistance in high-Mn content $Mn_{47+x}Ni_{43-x}Sn_{10}$ ferromagnetic shape memory alloys. J Appl Phys 2010; 108, 1–5.
[23] Kirat G, Kizilaslan O, Aksan MA. Magnetoresistance properties of magnetic Ni-Mn-Sn-B shape memory ribbons and magnetic field sensor aspects operating at room temperature. J Magn Magn Mater. 2019; 477, 366–371.
[24] Kirat G, Aksan MA, Aydogdu Y. Magnetic field induced martensitic transition in Fe doped Ni-Mn-Sn-B shape memory ribbons. Intermetall 2019; 111, 106493-106503.
[25] Sakon T, Sasaki K, Numakura D, Abe M, Nojiri H, Adachi Y, Kanomata T. Magnetic Field-Induced Transition in Co-Doped $Ni_{41}Co_9Mn_{31.5}Ga_{18.5}$ Heusler Alloy. Mater Trans 2013; 54, 9-13.
[26] Kainuma R, Imano Y, Ito W, Sutou Y, Morito H, Okamoto S, Kitakami O, Oikawa K, Fujita A, Kanomata T, Ishida K. Magnetic-field-induced shape recovery by reverse phase transformation. Nature 2006; 439, 957–960.
[27] Liu J, Scheerbaum N, Hinz D, Gutfleisch O. Magnetostructural transformation in Ni-Mn-In-Co ribbons. Appl Phys Lett 2008; 92, 35–38.
[28] Chen Z, Cong D, Li S, Zhang Y, Li S, Cao Y, Li S, Song C, Ren Y, Wang Y. External-field-induced phase transformation and associated properties in a $Ni_{50}Mn_{34}Fe_3In_{13}$ metamagnetic shape memory wire. Metals 2021; 11, 1–14.
[29] Brown PJ, Gandy AP, Ishida K, Kainuma R, Kanomata T, Neumann KU, Oikawa K, Ouladdiaf B, Ziebeck KRA. The magnetic and structural properties of the magnetic shape memory compound $Ni_2Mn_{1.44}Sn_{0.56}$. J Phys-Condens Mat 2006; 18, 2249–2259.